

Estimation of Decay Heat and Fission Product Release from a Molten Debris Pool

Jeong Ick Yun, Kune Y. Suh and Chang Sun Kang

Seoul National University
Department of Nuclear Engineering
San 56-1 Shinrim-dong, Kwanak-gu, Seoul, 151-742, Korea
Phone: +82-2-880-8324, Fax: +82-2-889-2688, Email: kysuh@plaza.snu.ac.kr

ABSTRACT

The debris pool may be formed in the reactor pressure vessel during a severe accident in the nuclear power plant. The fission product gas is activated and released from the debris pool as the pool temperature increases by decay power, while the less volatile fission products tend to remain as condensed phases because of their low vapor pressure. The release of noble gases and the volatile fission products is dominated by bubble dynamics. The diameter of the bubbles at detachment is calculated utilizing the Cole and Shulman correlation with the effect of system pressure. The release of the less volatile fission products from the pool can be analyzed based on mass transport through a liquid with the convection flow. Heat transfer is calculated at the curved bottom and at the top of the pool in partially filled hemispherical geometry. Also, the pool superheat is determined from the overall energy balance. Numerical analysis is performed for estimating released fraction of fission products from the debris pool and the rate of heat generation.

1. INTRODUCTION

During a severe accident in the nuclear power plant, as the reactor core material melts and relocates, the molten debris pool may be formed in the lower plenum of the reactor pressure vessel (RPV). Results of the TMI-2 accident analysis indicate that very little fission product release is expected from the rods and debris bed during formation of the molten pool. Rather, fission products can mostly be released from the molten pool. The molten pool is heated by the radioactive decay of the fission products trapped in the debris. Increase of the pool temperature will activate the fission product gas and result in release from the debris pool. In this study, focus was placed on the mechanisms of a fission product release from the oxidic pool. The volatile species (e.g., noble gases, I, Cs, etc.) in the pool have relatively high vapor pressure and may exist in concentration greater than their critical concentration in the pool. If the pressure and temperature in the pool are very high, as is the case of a station blackout (TMLB') for instance, the rate of nucleation and growth of bubbles is lower than at atmospheric system pressure. So, depressurization of the pool may significantly affect the nucleation and growth of the gas bubbles. In a previous experimental study [RASPLAV report, 1998], two layers with a distinct interface were found in the pool. The upper layer was porous and enriched in ZrO_2 , while the lower layer was enriched in UO_2 . However, for the sake of calculations, it is assumed that the pool is homogeneous.

2. FISSION FRODUCT RELEASE FROM THE POOL

2.1 Bubble Dynamics

The release of noble gases (Xe and Kr) and the volatile fission products (I and Cs) is dominated by bubble dynamics in the molten pool because these highly volatile fission products are gaseous at the high temperature (>2850 K) in the pool. As the pool heats up, fission product molecules are activated and thus the vapor pressure of the volatile fission products increases. If the vapor pressure exceeds the pool pressure, nucleation of the bubbles occurs. Nucleation of the bubbles may be explained by the homogeneous and the heterogeneous nucleation mechanisms. A simple configuration

for modeling is shown Figure 1. The nucleated bubbles have very small sizes and follow the natural convection flows. These bubbles will grow by coalescence diffusion of vapor molecules to bubbles. Small bubbles coalesce into larger bubbles by turbulence and differential bubble rise in the pool. Bubbles can be released from the pool as they sufficiently grow up. Bubble dynamics in the pool is thus characterized by bubble nucleation, coalescence, growth and rise. The time rate of change for the bubble concentration may be represented as follows

$$\frac{dn_i}{dt} = \frac{dn_{i,nucl}}{dt} + \frac{dn_{i,coal}}{dt} - \frac{dn_{i,loss}}{dt} + \frac{dn_{i,diff}}{dt} \quad (1)$$

2.1.1 Nucleation of a Bubble

Heterogeneous nucleation of a volatile fission product species will occur when the vapor pressure of the species minus the pool pressure exceeds the surface tension in the bubble-liquid surface:

$$P_g - P_m > (\sigma / R) \quad (2)$$

The number of nucleation sites can be assumed to be proportional to the number of solid particles in the melt. McClure et al. proposed that the total number of nucleation sites can be represented by summation of temperature-dependent nucleation sites and permanent nucleation sites. The permanent nucleation sites were assumed to exist on temperature-independent surfaces. The number of solid particles in the molten material is assumed to be proportional to the pool mass. The number of sites may be expressed as follows (McClure et al., 1993):

$$s_n = (m_p s_{n,t} + s_{n,p}) / V_P \quad (3)$$

For small cavity sizes, the bubble size at departure is dictated mainly by a balance between buoyancy and liquid inertial forces. But, for larger cavity sizes, the bubble size at departure is calculated by a balance of the surface tension and buoyant forces. A well-known equation was proposed by Fritz and Ende (1936) as

$$R_F = 0.0104 q_0 \sqrt{g / (g(r_l - r_v))} \quad (4)$$

This agreed well with the experimental data at atmospheric pressure, but did not concur with the experimental data at super- and sub-atmospheric pressures. Cole and Shulman (1966) found that, if $R_F = 0.5 \sqrt{g / (g(r_l - r_v))}$ for a contact angle of 48°, $R_d = R_d / R_F$ is a function of pressure. According to the experimental data, they obtained the following formula

$$\bar{R}_d = \frac{1000}{P} \quad (5)$$

where P is in mm Hg. The nucleation sites emit bubbles with a constant frequency. The frequency can be obtained by the time to grow to the departure diameter by diffusion. The time can be estimated by solving multi-component diffusion equation. Scriven (1959) proposed the following formulation for diffusion of a species to a sphere of changing radius

$$\sigma t \left(\frac{\partial r}{\partial t} - \frac{\kappa}{r} \right) = r^2 \frac{\partial \sigma}{\partial r} \quad (6)$$

The solution to Equation (7) is obtained as (Szekely and Martin, 1969) $\mathbf{V} = -a\mathbf{j}(\mathbf{b})$ where

$$\mathbf{j}(\mathbf{b}) = 2 \mathbf{b}_b^3 \exp(-3 \mathbf{b}_b^2) \times \int_0^\infty \mathbf{x}^{-2} \exp(-\mathbf{x}^2 - 2 \mathbf{b}_b^3 \mathbf{x}^{-1}) d\mathbf{x} \quad (7)$$

$$\mathbf{z} = \frac{C - C_m}{C_m} \quad \text{and} \quad a = D \frac{A}{C_m} \quad (8)$$

The growth constant \mathbf{b}_b can be obtained from Scriven's useful expression of solutions to equation (8)

$$\mathbf{j}(\mathbf{b}) \sim \sqrt{(\mathbf{p}/3)} [\mathbf{b} - 4/9 + 0(\mathbf{b}^{-1})] \quad (9)$$

Once \mathbf{b}_b is known, the bubble detachment frequency can be calculated as follows

$$f_d = \frac{1}{t} = \frac{4 \mathbf{b}_b^2 D}{R^2} \quad (10)$$

The product of the bubble detachment frequency and the number of nucleation sites determines the rate at which bubbles are formed, viz.

$$\frac{dn_{i,nucl}}{dt} = f_d \cdot s_n \quad (11)$$

2.1.2 Growth of a Bubble

Diffusion to a Bubble

Diffusion to a bubble is governed by Equation (7) used to calculate nucleation rate of the bubble. The rate of change of number density for bubble size R_i can be determined by the time to grow from bubble size R_{i-1} to size R_i . The rate of change of a discrete bubble radius R_i is the sum of loss term and production term. The loss term equals the number density of bubbles of size R_i divided by the time to grow from size R_i to size R_{i+1} and the production term is the number density of bubbles of size R_{i-1} divided by the time to grow from size R_{i-1} to size R_i . Therefore, the rate of change of number density for bubble size R_i is represented as:

$$\frac{dn_{i,diff}}{dt} = \frac{n_{i-1}}{t_i - t_{i-1}} - \frac{n_i}{t_{i+1} - t_i} \quad (12)$$

Coalescence of Bubbles

Bubbles interact due to their motion and grow by coalescence. The rate of coalescence of a bubble of radius R_k is given by Olander (1976) as

$$dn_k / dt = 0.5 \sum_{i+j=k} B_{ij} n_i n_j - \sum_{i=1} B_{ik} n_i n_k \quad (13)$$

The rate of change of number density for bubble size R_k can be obtained by summation of production term and loss term, too. The production term is represented by the rate of formation of bubble size R_k due to collisions of bubbles of sizes R_i and R_j . The loss term is represented by the rate of disappearance of bubble size R_k due to coalescence with bubbles of other sizes. It is assumed that bubble coalescence is caused by two mechanisms, i.e. turbulence in the pool and differential rise velocity of bubbles. For the turbulence process, a correlation for aerosol agglomeration in turbulent pipe flow is used as presented by Friedlander (1977)

$$B_{ij,turb} = 1.3(R_i + R_j)^3 (e_d / n)^{1/2} \quad (14)$$

where

$$e_d / n = (2 / R_p)(f / 2)^{1.5} v_{conv}^3 \quad (15)$$

The convective velocity in the pool can be obtained from an energy balance and is given by

$$v_{conv} = 2Q / (rA_{conv} c_p \Delta T), \quad (16)$$

For coalescence due to differential bubble rise velocity, the frequency function is also given by Friedlander (1977)

$$B_{ij,rise} = p(R_i + R_j)^2 |v_i - v_j| \quad (17)$$

For all the fission product release calculations, the molten pool is assumed to be a partially filled hemisphere. The material is (U, Zr)O₂ with a melting point at ~2850 K. It is assumed that the pool is homogeneous as described in the pervious section.

2.1.3 Loss of Bubbles due to Bubble Rise

The rate at which bubbles leave the pool is proportional to the bubble number density and rise velocity. The residence time of bubbles size R_k is given by height of the pool divided by the rise velocity. It is assumed that the rate at which bubbles leave the pool equals to the number density of bubbles divided by the residence time in the pool. The rise velocity of a spherical gas bubble is found by balancing the drag and buoyant forces on the bubble. Hence,

$$v = 2rgR^2 / 9m \quad (18)$$

The rate of the loss of bubbles due to buoyant rise can be calculated by:

$$\frac{dn_{i,loss}}{dt} = \frac{v_i n_i}{z} \quad (19)$$

2.2. Less-Volatile Fission Product Release

The less volatile fission products tend to remain as condensed phases in the melt because of their low vapor pressures. The chemical forms of the less volatile fission products in the melt are determined by the oxygen potential in the melt. It is assumed that mass transport governs release of the less volatile fission product from the pool. Rare earth elements such as europium and cerium exist as oxides, strontium is present as SrO, and ruthenium and antimony are present as metals immiscible in the molten pool (Petti, et al., 1989). The rate of mass transport of a species in a liquid is given by

$$M = k_m A_{up} (C_\infty - C_{surf}) \quad (20)$$

The mass transfer rate can be estimated by

$$dC / dt = -M / V_p = -(k_m A_{up} / V_p)(C_\infty - C_{surf}) \quad (21)$$

Diffusion can be estimated by means of a heat and mass transfer analogy. The mass transfer correlations for the top of the pool can be obtained as follows

$$Sh_{up} = 0.36 Ra^{0.23} (Sc/Pr)^{0.23} \quad (22)$$

2.3 Heat Transfer and Flow in a Molten Pool

Heat transfer and fluid flow in an oxidic pool shown in Figure 2 are induced by internal volumetric heat generated from the radioactive decay of fission product species retained in the pool. The pattern of flow in the pool having heat-generating liquid is depicted by natural convection being governed by a Rayleigh number characterizing the relationship between the forces of buoyancy and viscous friction. If the pool is deep enough, a stable natural-convection current can be formed. Kulacki and Goldstein suggest that convective mixing of the fluid produces a temperature profile that is axially and radially uniform, except for thin laminar boundary layers at the top and at the bottom (1972). Therefore, it is assumed that heat transfer in the pool can be treated with lumped parameter methods without introducing a significant error in the estimation of the pool temperature. Natural convection phenomena can be scaled in terms of the Grashof, Gr, and Prandtl, Pr, numbers. The presence of volumetric heating necessitates use of the Dammköhler, Da, number. These numbers are expressed (Theofanous, et al., 1994), respectively, as

$$Gr = \frac{g \beta (T_{max} - T_i) H^3}{\nu^2}, \quad Pr = \frac{\nu}{\alpha}, \quad Da = \frac{\dot{Q} H^2}{k(T_{max} - T_i)} \quad (23)$$

The Rayleigh number is given by $Ra = Gr \cdot Pr \cdot Da$ and the behavior of the overall heat transfer can be characterized by the correlations in the form of

$$Nu = f(Gr, Pr, Da) = C_A Ra^{C_B} \quad (24)$$

where C_A and C_B are empirically determined constants, and

$$Ra = \frac{b g \dot{Q} H^5}{\nu \alpha k} \quad (25)$$

For the oxidic pool, the ranges of the Ra and Pr numbers are, respectively
 $10^{15} < Ra < 6 \cdot 10^{15}$ $Pr \sim 0.6$

Using the best-known correlations, heat transfer is calculated at the curved bottom and the top of the pool. The correlations are summarized below (Mayinger, et al., 1976, Asfia, et al., 1994).

$$Nu_{up} = 0.36 Ra^{0.23} \quad (26)$$

$$Nu_{down} = 0.54 Ra^{0.2} (H/R_p)^{0.25} \quad (27)$$

The overall energy balance that equates the heat production rate to the heat loss rate is

$$V_p \dot{Q} = A_{up} q_{up} + A_{down} q_{down} \quad (27)$$

where A_{up} and A_{down} are surface areas of partially filled hemispherical geometry at each direction. In a partially filled hemisphere geometry, A_{up} and A_{down} can be determined as follows

$$A_{up} = \pi R_p^2 (1 - x^2) \quad (28)$$

$$A_{down} = 2\pi R_p^2 \cos(\arcsin x) \quad (29)$$

$$x = 1 - H/R_p \quad (30)$$

Substituting Equations (23) and (24) into Equation (25) to eliminate q_{up} and q_{down} , the pool superheat ΔT is calculated by

$$\Delta T = \frac{H V_p \dot{Q}}{k} [0.54 A_{up} (Ra)^{0.2} (H/R)^{0.25} + 0.36 A_{down} (Ra)^{0.23}] \quad (31)$$

Decay heat of fission products in the pool is calculated as:

$$\dot{Q} = \sum_i M_i(t) \mathbf{h}(i) \quad (32)$$

At a time t , initial mass concentration of fission product i in the pool can be obtained by

$$M_{i,0}(t) = [M_{i,j} + (M_{i,j+1} - M_{i,j}) \frac{(t - t_j)}{(t_{j+1} - t_j)}] (1 - f_c) (m_c / m_p) \quad (33)$$

In above equation, $M_{i,j}$ and t_j are tabular output of ORIGEN 2 code. Using the ORIGEN 2 code, the initial core inventories and pool inventories at each time can be estimated.

3. RESULTS AND DISCUSSION

For all the fission product release calculations in this work, the main parameters were obtained from the analysis reports of the TMI-2 accident (Akers, et al., 1989). The pool is assumed to be a partially filled hemisphere, 1.45 m in radius and 32,700 kg in mass. The change of pool geometry during the numerical calculation is neglected. The fission product inventories in the pool are about 24.5% of the total core inventories. The parameters used in the calculations are

listed in Table 1. From the numerical analysis, the height of the pool is 1.014 m and peak temperature at the pool center exceeds 3300 K. Physical properties of the molten pool are given by temperature-dependent correlations.

For the calculation of heat generation rate in the pool, twenty- nine (29) elements were chosen and classified in Table 2. Note that decay power fraction of the remaining elements except the 29 elements is less than 1%. The released fraction of each fission product is calculated by bubble dynamics and mass transport. From concentrations of the 29 elements in the pool, the heat generation rate is obtained at time t . As the fission products are released from the pool, the peak temperature slightly decreased. At figure 3 and 4, peak temperature and rate of heat generation in the pool are compared. When release of the fission product from the pool is considered, Peak temperature of the pool decreases from 3228 to 3164 K at 4000 second.

Sensitivity analyses for the fission product release model were performed. Results for the number of temperature-dependent nucleation sites of 1,000 and 5,000 are shown in Figure 5. The released fraction at 1,000 sec highly increases from ~ 0.4 to ~ 0.8 with the increase in the number of sites. In the previous study, McClure et al. (1993) determined the parameters for which variations in their values have the greatest impact on the calculated rate of fission product release. These were the number of nucleation sites in the pool and the diffusivity of the pool. The results presented in Figure 5 agree with the their results.

Effects on the released fraction of fission products were estimated for surface tension of the pool and the pool pressure. Bubble radius at detachment is determined with the Cole and Shulman (1966) correlation. If the pool pressure is 10 MPa, the initial bubble radius with the Fritz and Ende (1936) equation is up to 3 \sim 71 times that calculated with the Cole and Shulman correlation. Also, diffusion to a bubble is significantly reduced than at the atmospheric pressure. As depicted in Figure 6, the time to release 99% of the pool inventory is 1140 sec at 5 MPa of system pressure and 1890 sec at 10 MPa. These results suggest that the pool pressure has a major effect on the fission product release.

The size of a nucleated bubble varies with surface tension. From Equation (5), the bubble size at detachment R_d is proportional to \sqrt{g} . Also, growth to larger bubble is affected by increase of surface tension. Figure 7 shows that time to release 90% of inventory is slightly shorter than \sqrt{g} .

The time to release 90% of the pool inventory calculated by nucleation, coalescence, diffusion to a bubble and loss due to bubble is up to 3~100 times that estimated by bubble coalescence only (Petti et al., 1989). In this study, the time to release 90% of the total inventory was estimated to be greater than 1,000 sec. Petti et al. suggest that most of the gas would be released from the pool very quickly, say, within 5 min, on the other hand.

4. CONCLUSIONS

Based on the numerical analysis of fission product behavior, following conclusions can be drawn concerning the release of fission products. A large amount of volatile fission products shall be released during formation of the molten pool. It is concluded that time to release 90% of inventory, at least, takes more than 1,000 sec. But results of all the calculations indicate that large amount of volatile fission products would be released from the pool during phase 3b (between 180 and 224 min after reactor shutdown). As shown from the sensitivity analysis results, the change in the pool pressure significantly affects the nucleated bubble radius, rate of bubble growth, and fission product release. Therefore, the change of the system pressure during formation of the molten pool should be considered for the fission product release from the pool. The release of fission products would be mainly governed by the number of nucleation sites in the pool, surface tension of liquid in pool, diffusivity of fission product in pool and pressure in pool.

NOMENCLATURE

A = area of bubble surface	$[m^2]$
A_{conv} = area for convection	$[m^2]$
A_{down} = area for downward heat transfer	$[m^2]$
A_{up} = area for upward heat transfer	$[m^2]$
B = coalescence frequency function	$[m^3/s]$
C = fission product concentration in the pool	$[No./m^3]$
c_p = heat capacity	$[W/mK]$
D = diffusivity of the fission product in the pool	$[m^2/s]$
f = Fanning friction factor (0.004)	
$f_{c,i}$ = released fraction of species i in the core	
f_d = bubble detachment frequency	$[s^{-1}]$
f_m = molten fraction of the pool	
H = pool depth	$[m]$
k = thermal conductivity	$[W/m \cdot K]$
m_c = mass of the core	$[kg]$
m_p = mass of the pool	$[kg]$
n = number density of bubble	$[No./m^3]$
s_n = number density of nucleation site	$[site/kg]$
$s_{n,p}$ = number of permanent nucleation sites	$[site/kg.]$
$s_{n,t}$ = number of temperature-dependent nucleation sites	
P_g = pressure of gas bubble	$[N/m^2]$
P_m = pressure of the pool	$[N/m^2]$
\mathcal{Q} = volumetric heat generation rate	$[W/m^3]$
q = average heat flux over a boundary	$[W/m^2]$
R = radius of bubble	$[m]$
R_d = radius of bubble at departure	$[m]$
R_p = radius of the molten pool	$[m]$
T = temperature of the pool	$[K]$
ΔT = pool superheat	$[K]$
V_p = volume of the pool	$[m^3]$
v = velocity of bubble	$[m/s]$

Greek Letters

\mathbf{a} = thermal diffusivity	$[m^2/s]$
\mathbf{b} = thermal expansion coefficient	$[K^{-1}]$
\mathbf{b}_b = growth constant of diffusion to a bubble	
\mathbf{g} = bubble-melt interfacial tension	$[N/m]$
\mathbf{h} = heat generation per unit mass	$[W/kg]$
\mathbf{e}_d = eddy diffusivity	$[m^2/s^3]$
\mathbf{k} = gas constant (Boltzmann constant)	$[J/K]$
\mathbf{q}_0 = contact angle of nucleating bubble	$[degree]$
\mathbf{n} = kinematic viscosity	$[kg/m \cdot s]$
\mathbf{r}_m = density of the pool	$[kg/m^3]$
\mathbf{m} = viscosity of the pool	$[N \cdot s/m^2]$

Subscripts

i = bubble size bin i
j = bubble size bin j
k = bubble size bin k
0 = initial value or nominal value
coal = coalescence
conv = convection
diff = diffusion
nucl = nucleation
loss = loss due to bubble rise

REFERENCES

- Asfia, F. J., B. Frantz and V. K. Dhir, "Experimental Investigation of Natural Convection in Volumetrically Heated Spherical Segments," Submitted to J. of Heat Transfer, 1994.
- Cole, R., H. L. Shulman, "Bubble Departure Diameters at Subatmospheric Pressures," Chemical Engineers Progress Symposium Series 62, Vol. 64, p6-16, 1966.
- Friedlander, S. K., "Smoke, Dust and Haze: Fundamentals of Aerosol Behavior," John Wiley and Sons, New York, NY. USA, 1977.
- Fritz, W., W. Ende, "Über den Verdampfungsvorgang nach Kinematographischen Aufnahmen an Dampfblasen," Physik Zeitscher, Vol.37, p391-401, 1936.
- Kulacki, F. A., and R. J. Goldstein, "Thermal Convection in a Horizontal Fluid Layer with Uniform Volumetric Energy Sources," J. Fluid Mech., Vol. 55, Part 2, p 271, 1972.
- Mayinger, F., et al. "Examination of Thermohydraulic Processes and Heat Transfer in a Core Melt," Final Report BMFT RS 48/1, Hannover Technical University, Germany, 1975.
- McClure, P. R., M. T. Leonard and A. Razani, "A Model for Fission Product Release from Liquid-Metal Pools: Development and Sensitivity Investigation," Nuclear Science and Eng., Vol. 114, p 102-111, 1993.
- Olander, D. R., "Fundamental Aspects of Nuclear Reactor Fuel Elements," TID-26711-P1, Department of Energy, Washington, DC, USA, 1976.
- Petti, D. A., et al., "Analysis of Fission Product Release Behavior from the Three Mile Island Unit 2 Core," Nuclear Technology, Vol. 87, p 243-263, August 1989.
- Scriven, L. E., "On the Dynamics of Phase Growth," Chem. Eng. Sci., Vol. 10, pp. 1, 1959.
- Theofanous, T.G., et al., "In-Vessel Coolability and Retention of A Core Melt," DOE/ID-10460, 1994.
- "Behavior of Corium Melt Pool Under External Cooling," Final Report of the First Phase of RASPLAV Project, Kurchatov Institute, Russia, January 1988.

Table 1 Values and Ranges of Parameters

Parameter	Value
Pool mass, M_p [kg]	32,700
Pool radius, R_p [m]	1.45
Pool pressure, p [MPa]	0.1 ~ 10.0
Pool velocity, V_{conv} [m/sec]	0.13
Number of permanent nucleation sites [site/kg]	100 ~ 1000
Number of temperature-dependent nucleation sites [site/kg]	100 ~ 30,000
Diffusivity of fission product [m ² /sec]	1×10^{-11} ~ 1×10^{-7}
Surface tension of liquid in pool σ [N/m]	0.5 ~ 1.6

Table 2 Radionuclide Elements and Classes

Class	Member Elements
1. Noble gases	Xe, Kr
2. Alkali metals	Cs, Rb
3. Alkaline earths	Ba, Sr
4. Halogens	I, Br
5. Chalcogens	Te, Se
6. Platinoids	Ru, Pd, Rh
7. Transition metals	Mo, Tc, Nb
8. Tetravalents	Ce, Zr, Np
9. Trivalents	La, Pm, Y, Pr, Nd
10. Uranium	U
11. More volatile metals	As, Sb
12. Less volatile metals	Sn, Ag

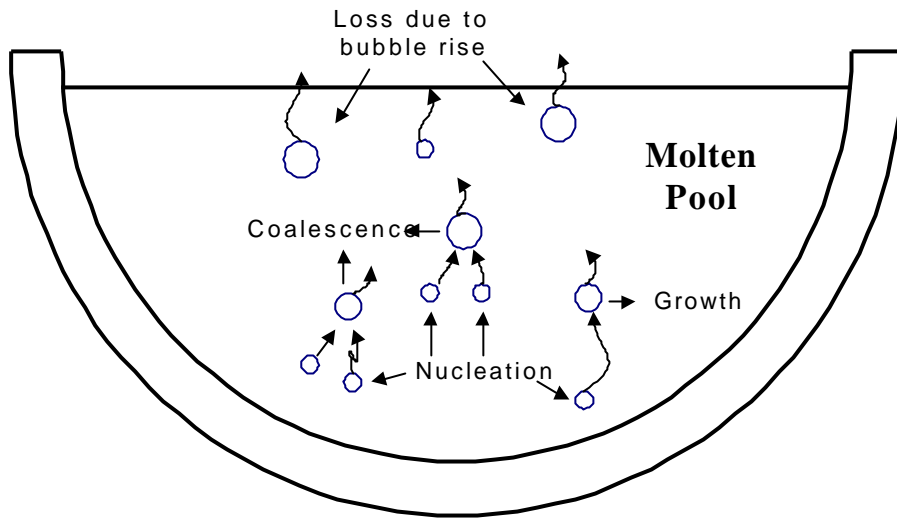


Fig. 1 Bubble dynamics in a molten pool

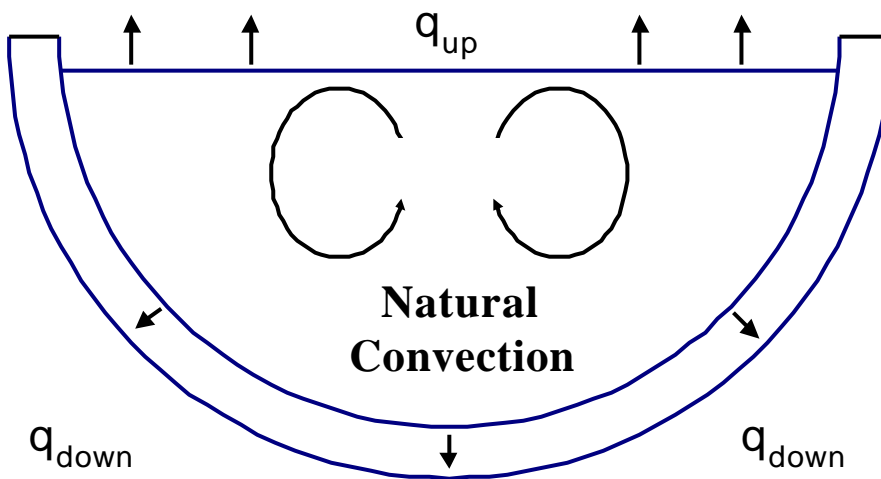


Fig. 2 Heat transfer and fluid flow in a molten pool

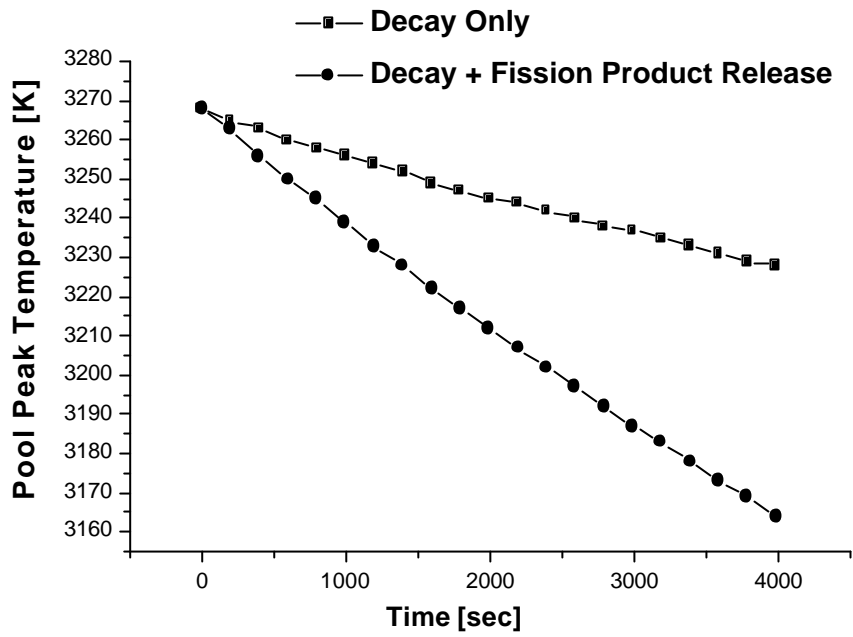


Fig 3 Pool peak temperature with and without the release

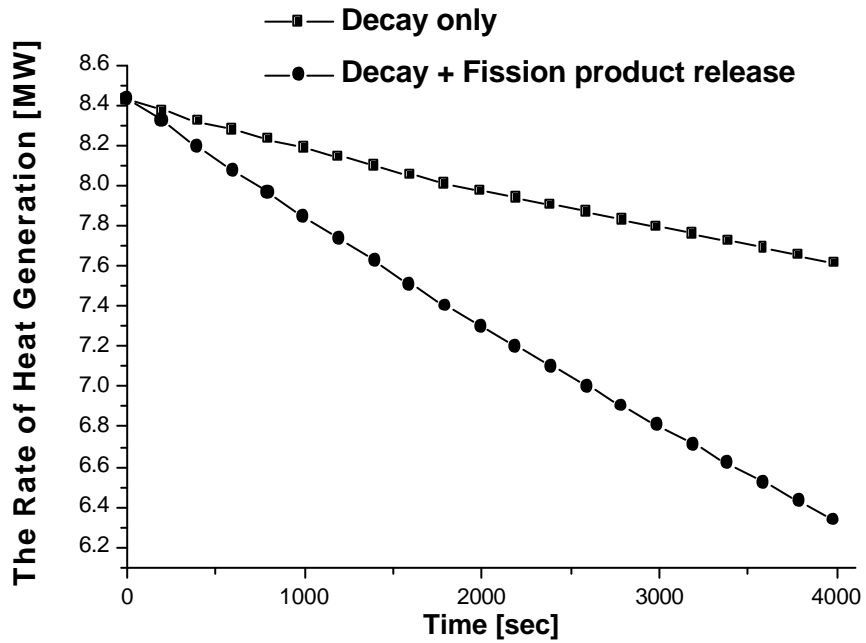


Fig 4 Decay heat in the pool, with and without the release

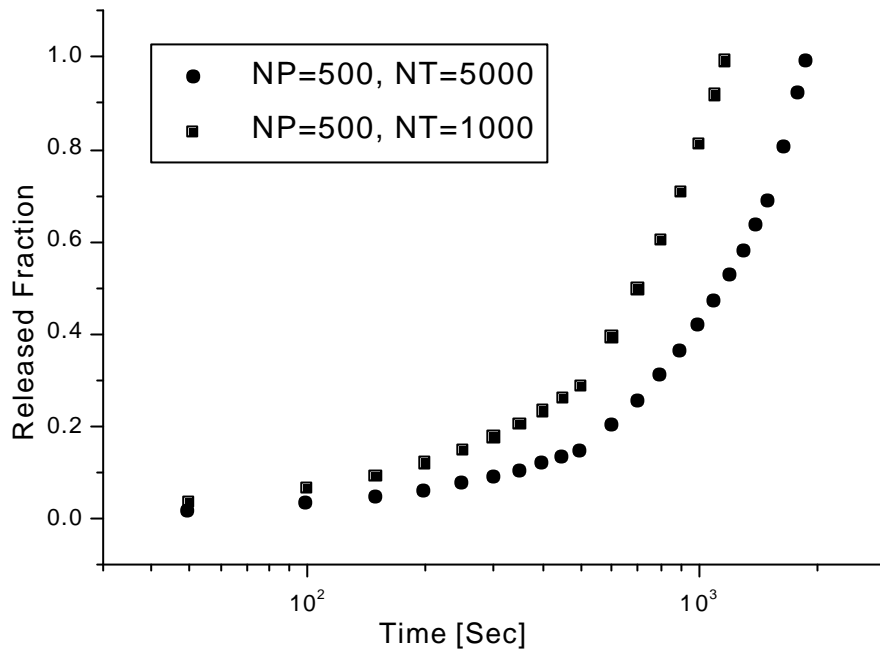


Fig 5 Released fraction for number of nucleation sites

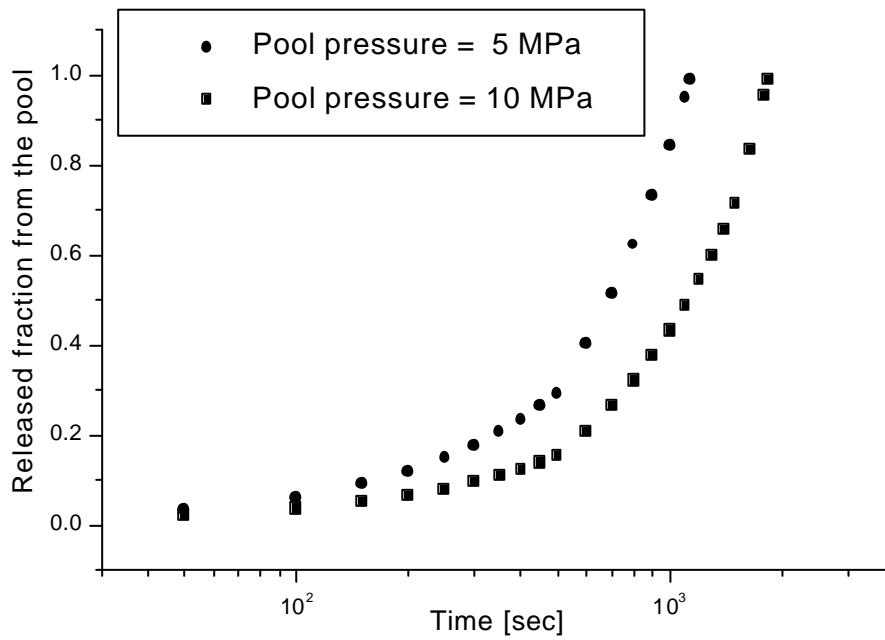


Fig 6 Released fraction at the high pool pressure

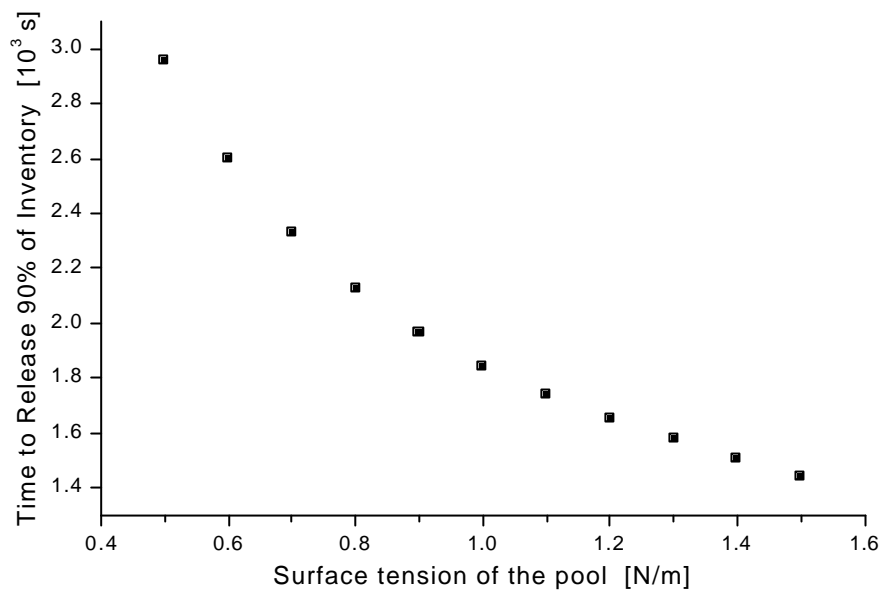


Fig 7 Release time vs surface tension